Localized Excitations and the Geometry of the $^1n\pi^*$ Excited States of Pyrazine

Daniel A. Kleier,[1a-c] Richard L. Martin,*[1a] Willard R. Wadt,[1a] and William R. Moomaw[1b]

Contribution from the Theoretical Division, MS 569, Los Alamos National Laboratory, Los Alamos, New Mexico 87545, and Department of Chemistry, Williams College, Williamstown, Massachusetts 01267. *Received June 22, 1981*

Abstract: Previous theoretical work has shown that the lowest excited singlet state of pyrazine, the $n\pi^*$ $^1B_{3u}$ state, is best described in terms of interacting excitations localized on each nitrogen. The present work refines the localized excitation model and considers its implications for the geometry of the $^1B_{3u}$ state. Hartree-Fock calculations show that the best single configuration description of the $n\pi^*$ state has broken ($^1B_1$) symmetry with the excitation strongly localized at one end of the molcule. If the symmetry-restricted HF result is used for reference, this localization describes an important correlation effect. The excited-state geometry was probed using configuration interaction wave functions based on the symmetry-restricted orbitals, as well as properly symmetrized "valence-bond" wave functions based on the broken symmetry solutions. Both descriptions lead to a very flat potential for a b_{1u} vibrational mode. This mode reduces the molecular geometry from D_{2h} to C_{2v}. We present spectroscopic evidence of our own and of other workers which is consistent with such a flat potential.

I. Introduction

In many applications of the Hartree-Fock (HF) method,[2] orbital symmetry restrictions are adopted as a matter of convenience and computational ease. Molecular orbitals (MOs) are routinely required to transform according to one of the irreducible representations of the molecular point group. In the vast majority of cases these symmetry restrictions are justified, as evidenced by the symmetry properties of the canonical MOs[3] (CMOs) when the restrictions are relaxed. However, several examples are now known for which the CMOs for the best single configuration wave function break symmetry.[4-6] That is, the CMOs transform according to an irreducible representation of a *sub*group of the full symmetry group of the molecule.

Wadt and Goddard[4] first observed this behavior in the lowest lying singlet excited state of pyrazine. In the standard symmetry-restricted MO picture the $^1B_{3u}$ state arises from an excitation from the $n_+(a_g) = (n_l + n_r)$ combination of lone-pair orbitals[7] into the lowest lying π^* (b_{3u}) orbital,[7] while excitation from the $n_-(b_{1u}) = (n_l - n_r)$ combination of lone-pair orbitals leads to the $^1B_{2g}$ state. However, when symmetry restrictions are relaxed, each state is represented by a broken symmetry HF solution, which transforms according to B_1 representation of the $C_{2v}(z)$ subgroup of D_{2h} (i.e., the excitation is largely localized on one nitrogen as in Φ_r or Φ_l of Figure 1).[8] Even though the localized solutions do not possess the full symmetry of the true wave function, they give an energy which is 1.1 eV lower than the symmetry-restricted HF (SRHF) description.[4,5m,9,10]

Does the broken electronic symmetry described above imply a preference by the nuclei for a lower symmetry? In the case at hand, one of the ways in which the nuclear geometry can be reduced from D_{2h} to C_{2v} is by opening one CNC angle while closing the other. This nontotally symmetric b_{1u} vibrational mode is dipicted in Figure 2. The b_{1u} mode will mix the $^1B_{3u}$ and $^1B_{2g}$ states through a second-order Jahn-Teller (SOJT) coupling,[11] and thus the lower of these two states (i.e., the $^1B_{3u}$ state) could conceivably be characterized by a double-well potential along the b_{1u} normal coordinate. The computations in this paper attempt to assess the validity of this hypothesis.

Evidence for molecular distortions will also be sought from published spectral data. Azumi[12] has proposed molecular distortions in the pyrazine triplet $n\pi^*$ state, but he interprets his phosphorescence spectra in terms of a reduction to C_{2h} [$C_2(y)$]. Two-photon spectra in both the vapor[13] and crystal[14] phases and

(1) (a) Los Alamos National Laboratory; (b) Williams College; (c) Dreyfus Teacher-Scholar, 1979-1984.

(2) Abbreviations used in this manuscript: AO, atomic orbital; CI, configuration interaction; CMO, canonical molecular orbital; DZ, double zeta; HF, Hartree-Fock; LCAO, linear combination of atomic orbitals; MBS, minimal basis set; MO, molecular orbital; POL(1) CI, all singles and doubles CI with no more than one electron outside the valence space; PSUHF, projected symmetry unrestricted Hartree-Fock; SOJT, second-order Jahn-Teller; SRHF, symmetry restricted Hartree-Fock; STO-3G, Slater-type orbital represented by three Gaussians; SUHF, symmetry unrestricted Hartree-Fock; VB, valence bond; (1+2) CI, all singles and doubles CI.

(3) R. McWeeney and B. T. Sutcliffe, "Methods of Molecular Quantum Mechanics", Academic Press, New York, 1969.

(4) (a) W. R. Wadt and W. A. Goddard, *J. Am. Chem. Soc.*, **97**, 2034 (1975); (b) W. R. Wadt, W. A. Goddard, and T. H. Dunning, *J. Chem. Phys.*, **65**, 438 (1976).

(5) A sampling of recent studies includes: (a) C. P. Keijzers, P. S. Bagus, and J. P. Worth, *J. Chem. Phys.* **69**, 4032 (1978) [pyromellitic acid dianhydride); (b) H. C. Longuet-Higgins and L. Salem, *Proc. R. Soc. London, Ser. A*, **251**, 172 (1959) (long-chain conjugated molecules); (c) G. Chambaud, B. Levy, and P. Millie, *Theor. Chim. Acta*, **48**, 103 (1978) (O_2^{2-}); (d) L. E. Nitzsche and E. R. Davidson, *Chem. Phys. Lett.*, **58**, 171 (1978) ($^3n\pi^*$ states of glyoxal); (e) C. F. Jackels and E. R. Davidson, *J. Chem. Phys.*, **64**, 2908 (1976) (NO_2 radical); (f) J. Paldus and A. Veillard, *Mol. Phys.*, **35**, 445 (1978) (allyl radical); (g) B. Y. Simkin, M. N. Glukhovtsev, and V. I. Minkin, *Chem. Phys. Lett.*, **71**, 284 (1980) (1,4-dihydroquinoxalinedione-5,8 and its heteroanalogues); (h) A. D. McClean, Seventh Canadian Symposium on Theoretical Chemistry, June 1980 (formyloxy radical); (i) W. C. Nieuwpoort and R. Broer, in footnote h ($n-\pi^*$ states of *p*-benzoquinone); (j) W. G. Laidlaw, and K. Vasudewan *Theor. Chim. Acta*, **26**, 387 (1972) (pentalene and heptalene); (k) W. G. Laidlaw, *Int. J. Quantum Chem.*, **7**, 87 (1973) (nonalternant hydrocarbons); (l) A. Toyota, T. Tanaka, and T. Nakajima, *ibid.*, **10**, 917 (1976) (conjugated hydrocarbons); (m) S. Canuto, O. Goscinski, and M. Zerner, *Chem. Phys. Lett.* **68**, 232 (1979) (pyrazine); (n) J. Müller, E. Poulain, O. Goscinski, and l. Karlsson, *J. Chem. Phys.*, **72**, 2587 (1980) (carbon tetrafluoride); (o) L. Engelbrecht and B. Liu, Abstracts, 2nd Annual West Coast Theoretical Conference, Pasadena, CA 1980 (CO_2); (p) L. Noodleman and J. G. Norman *J.* Chem. *Phys.*, **70**, 4903 (1979) ($Mo_2Cl_8^{2-}$); (q) Y. Yamaguchi, *Chem. Phys. Lett.* **68**, 477 (1979) ($Mo_2Cl_8^{2-}$); (r) R. F. Fenske and J. R. Jensen, *J. Chem. Phys.* **71**, 3374 (1979) (MnNO, CoNO); (s) M. Benard, *J. Chem. Phys.*, **71**, 2546 (1979) ($Mo_2(O_2CH)_4$; (t) D. A. Kleier and W. N. Lipscomb, *Inorg. Chem.*, **18**, 1312 (1979) ($B_8H_8^{2-}$).

(6) (a) J. Paldus and J. Cizek, *J. Polym. Sci., Part C*, 199 (1970); (b) *J. Chem. Phys.*, **52** 2919 (1970); (c) *Ibid.*, **47**, 3976 (1967); (d) P. O. Lowdin, *Rev. Mod. Phys.*, **35**, 496 (1963); (e) *Adv. Chem. Phys.*, **14**, 283 (1969); (f) H. F. King and R. E. Stanton, *J. Chem. Phys.*, **50**, 3789 (1969).

(7) n_l and n_r designate nonbonding orbitals on the left- and right-hand nitrogens, respectively. π_l and π_r denote π orbitals on the left and right nitrogens. This article deals only with states corresponding to excitation from one of the lone-pair orbitals into the antibonding orbital of b_{3u} or b_1 symmetry. Thus, within the confines of this article π^* will be used to denote this specific orbital and should not be taken in its more generic sense.

(8) (a) In localized solution Φ_r, the singly occupied nonbonding orbital is localized on the right-hand nitrogen while the singly occupied π orbital is localized on the atoms para and ortho to the right nitrogen. An underlying doubly occupied π orbital is also localized on the right nitrogen. (b) It should be emphasized that the full spin restrictions were imposed on the wave functions, only the spatial symmetry constraints were relaxed.

(9) R. L. Martin, *J. Chem. Phys.*, **74**, 1852 (1981).

(10) M. Hackmeyer and J. L. Whitten, *J. Chem. Phys.*, **55**, 3739 (1971).

(11) (a) R. G. Pearson, "Symmetry Rules for Chemical Reactions", Wiley, New York, 1976, pp 12-17. (b) L. S. Bartell, *J. Chem. Educ.*, **45**, 754 (1968).

(12) K. Matsuzaki and T. Azumi, *J. Chem. Phys.*, **69**, 3907 (1978).

(13) I. Knoth, H. J. Neussor, and E. W. Schlag, *Z. Naturforsch. A.*, **34**, 979 (1978).

0002-7863/82/1504-0060$01.25/0

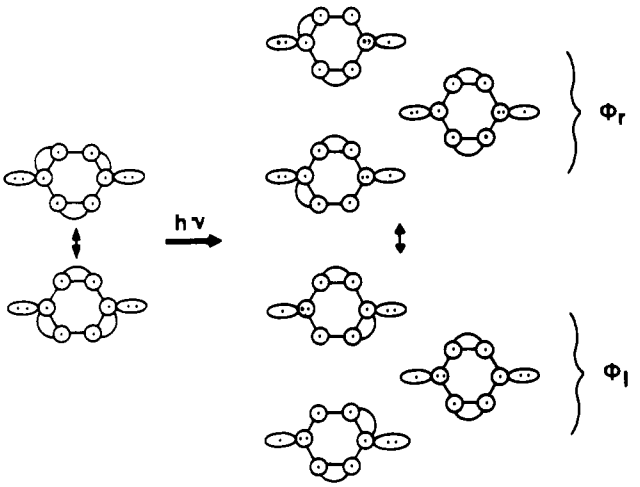

Figure 1. Resonance structures for ground and $n\pi^*$ excited states of pyrazine. The circles denote $p\pi$ orbitals perpendicular to the plane of the paper, and the ellipses the nonbonding σ orbitals on the nitrogens. Electrons are represented by dots and are shown coupled into the two VB Kekulē structures on the left. The tie lines indicate a pair of orbitals singlet coupled into a π bond. Φ_r and Φ_l are resonance structures corresponding to the localized solutions with excitations on the right- and left-hand nitrogens, respectively.

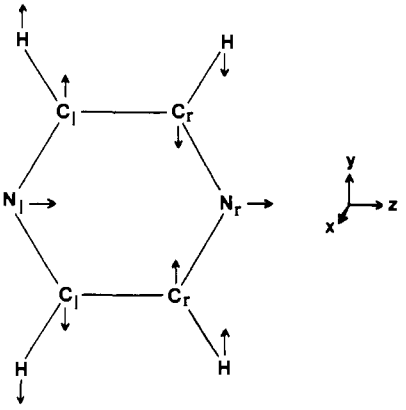

Figure 2. b_{1u} mode of distortion. The depicted displacements are with respect to the optimal D_{2h} structure.

one-photon spectra in strongly hydrogen-bonding solvents[15] bear more directly on the question of molecular distortions in the singlet state.

II. Methods

A. Geometry Optimizations, Basis Sets, and Hartree–Fock (HF) Calculations. All geometry optimizations were performed at the single-determinant level using a minimal basis set (MBS) of STO-3G orbitals.[16] Optimization modes included those which varied the CC and CN bond distances as well as the CNC angles. The CH bond distances were held fixed at 1.09 Å and variations of the hydrogen atom positions were parallel to those of the carbon atoms with which they were associated. The optimal $^1B_{3u}$ geometry (designated Opt $^1B_{3u}$) is defined by the energy minimum of the D_{2h} symmetry-restricted wave function. The nuclei of the optimal $^1B_1$* geometry (designated Opt $^1B_1$*) also possess D_{2h} symmetry, but the electronic wave function used in the optimization transforms according to the B_1 representation of the C_{2v} subgroup. The optimal C_{2v} geometry for the first $n\pi^*$ state is designated Opt $^1B_1$. Thus, the "Opt $^1B_1$" and "Opt $^1B_1$*" geometries differ in that the former is a C_{2v} geometry and the latter a D_{2h} geometry though both were optimized using a wave function of $^1B_1$ species. Geometries along the vibration coordinate of b_{1u} symmetry were calculated using a least motion path[17] defined by the optimal D_{2h} and $C_{2v}(z)$ geometries as end points.

The basis employed in the DZ calculations was a set of [3s,2p/2s] functions contracted[18] from Huzinaga's[19] (9s,5p/4s) set of primitive Gaussian functions. The hydrogen exponents were not scaled though they have been in previous work.[4]

All open-shell HF calculations were performed with the GVBTWO program.[20a] The broken-symmetry SCF solutions (designated 1^1B_1 and 2^1B_1)[21] for the D_{2h} geometries were obtained by using starting orbitals which transformed according to species of the $C_{2v}(z)$ point group. The two nonequivalent localized solutions for the $n\pi^*$ states of pyrazine in a C_{2v} geometry were obtained by first solving self-consistently for the lower energy member of the pair, 1^1B_1. The converged orbitals for the 1^1B_1 state were then "reflected"[22] to generate an initial guess for the 2^1B_1 state. Once a converged set of orbitals was obtained in this manner for the 2^1B_1 state, it was used as an initial estimate for further calculations of this state.

B. Configuration Interaction Calculations. Each CI calculation[20b] was based upon orbitals from the HF calculation for the state of interest (e.g., for a D_{2h} geometry the CI on the 1^1B_1 state used broken symmetry orbitals while CI calculations on the $^1B_{3u}$ state used the appropriate symmetry restricted orbitals). For the CI calculations in the extended virtual space of the DZ basis, the following partitioning technique was used.

(a) The unoccupied orbitals of the MBS space were transformed by replacing the AOs of the LCAO expansions with their scaled DZ counterparts.[23] Designate this new set of unoccupied valence orbitals as $\{\Phi_i(\text{MBS}\rightarrow\text{DZ})\}$.

(b) Each orbital of $\{\Phi_i(\text{MBS}\rightarrow\text{DZ})\}$ was used to replace the orbital of the extended virtual space which it most closely resembled (by inspection).

(c) The $\{\Phi_i(\text{MBS}\rightarrow\text{DZ})\}$ set was Schmidt orthogonalized to the occupied orbitals. These orbitals are the valence or inner virtual orbitals of the partitioned space. The remaining virtual orbitals were then orthogonalized to the valence orbitals (occupied + virtual) and are designated as the outer virtual orbitals.

In the MBS space, CI calculations with all single and double excitations ((1+2) CI) from either one or two leading configurations were performed. The partitioning described above was utilized to perform POL(1) CIs in the extended space. The POL(1) CIs included all single and double excitations from either one or two leading configurations with no more than one electron outside the valence space. Several of the above CI calculations slightly exceeded the limit of ~11 500 spin eigenfunctions imposed by the computer code.[20b] Thus, relatively small linear extrapolations based upon perturbation theory were performed to obtain the CI energies at the desired level of correlation. With only one exception the lengths of these extrapolations were less than 0.03 eV.

(14) P. Esherick, P. Zinsli, and M. A. El-Sayed, *Chem. Phys.*, **10**, 415 (1975).
(15) W. R. Moomaw, S. Vlasak, J. Kinney, and J. Cordes, manuscript in preparation.
(16) W. J. Hehre, R. F. Stewart, and J. A. Pople, *J. Chem. Phys.*, **51**, 2657 (1969).
(17) T. A. Halgren, and W. N. Lipscomb, *Chem. Phys. Lett.*, **49**, 225 (1977).
(18) T. H. Dunning, Jr., and P. J. Hay, in "Modern Theoretical Chemistry, II. Electronic Structure: *Ab Initio* Methods", H. F. Schaefer III, Ed., Plenum, New York, 1975.
(19) S. Huzinaga, *J. Chem. Phys.*, **42**, 1293 (1965).
(20) (a) F. W. Bobrowicz and W. R. Wadt, as described by F. W. Bobrowicz and W. A. Goddard in "Methods of Electronic Structure Theory", H. F. Schaefer, Ed., Plenum, New York, 1977; (b) F. W. Bobrowicz, CIPGM program written for CI calculations.
(21) We use 1^1B_1 to designate the lower of the two states, Φ_r or Φ_l (Figure 1). 2^1B_1 then designates the higher energy member of this pair. The identification of Φ_r or Φ_l with 1^1B_1 depends upon the sense of the b_{1u} distortion (see Figure 4 and text).
(22) The reflected molecular orbital ψ_i' is obtained from $\psi_i = \sum_j C_{ji}\phi_j$ by replacing the coefficient of each right-hand atomic orbital ϕ_{jr} with the coefficient of its partner under reflection ϕ_{jl}

$$\phi_{jr} \xrightarrow{\sigma} \phi_{jl}$$

and vice versa.
(23) P. J. Hay, private communication of atomic calculations on C(^{3}P) and N(^{4}S) states using a (9s,5p)/[3s,2p] basis of contracted Gaussian orbitals.

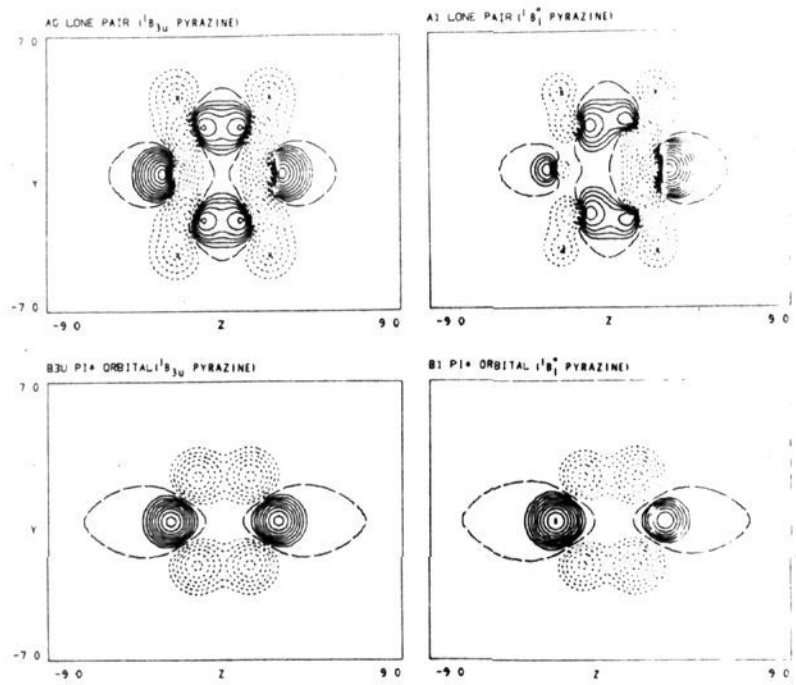

Figure 3. Contour plots of the singly occupied orbitals from the $^1B_{3u}$ and 1^1B_1 wave functions of pyrazine calculated at the MBS level. The ratio between consecutive contour levels is 1.58. Proceeding clockwise from the upper left, the most positive contours are at 0.80, 1.26, 0.80, and 0.50 au. The lone-pair contours are plotted in the plane of the molecule while the π^* orbitals are plotted in a plane 0.6 au above that of the molecule.

C. Valence-Bond Calculations. Valence-bond (or more precisely projected symmetry unrestricted Hartree–Fock (PSUHF)[8b]) calculations were performed by diagonalizing the 2 × 2 Hamiltonian between the nonorthogonal functions (1^1B_1 and 2^1B_1) which correspond to excitations localized on opposite ends of the molecule. These calculations were made possible by first transforming the two sets of localized orbitals, $\{\phi_i^l\}$ and $\{\phi_i^r\}$, into sets of corresponding orbitals,[24] $\{\phi_i^{l'}\}$ and $\{\phi_i^{r'}\}$, which are orthogonal in the sense that $\int \phi_1^r \phi_j^{1'} d\tau = \lambda_{ij}\delta_{ij}$ where $\lambda_{i_j} \leq 1$. Evaluation of off-diagonal elements of the Hamiltonian are greatly facilitated by this tranformation, the details of which are described elsewhere.[9]

III. Results

The localized resonance structures from the symmetry-unrestricted HF (SUHF) calculations have the $n\pi^*$ excitation localized on either the left- or right-hand nitrogen (Figure 1). The degree of localization is perhaps best appreciated by comparing contour plots for the singly occupied n and π^* orbitals of the symmetry-restricted HF (SRHF) wave function with those of the SUHF wave function for the same D_{2h} nuclear geometry (Figure 3). The SUHF nonbonding orbital is more than 90% localized on the right nitrogen while the π^* orbital is largely found on the left nitrogen. Compensating rearrangements in the underlying doubly occupied orbitals prevent any large asymmetric buildup of charge.

Our computed excitation energies are reported in Table II. When the excitation is allowed to localize, the computed vertical excitation energy (4.04 eV for the experimental ground-state geometry) shows the expected improved[4] agreement with the experimental value of 3.8–3.9 eV.[25] Although not included in this table, HF calculations at the MBS level yielded qualitatively similar results.

The results of the geometry optimizations are given in Table I, and for comparison the experimental geometry is also given. The only notable difference between the Exp and Opt ^1A_g geometries is the smaller experimental CN distance. Compared with the optimal ^1A_g geometry, the rings of the $^1B_{3u}$ and $^1B_1$* geometries are generally expanded and the CNC angles open by about 4°. An increase in the CNC angles of the $^1B_{3u}$ state is consistent with the conclusions of Thakur and Innes[26] which are based upon rotational analysis of the $10a_0^1$ vibronic band of the $^1B_{3u} \leftarrow {}^1A_g$ transition. The ring expansion of the Opt $^1B_{3u}$ geometry results from the elongation of the CC bonds, while the expansion of the Opt $^1B_1$* geometry is principally due to the elongation of the CN bonds. The most striking characteristic of the Opt $^1B_1$ geometry is the large difference of 13° between the CNC angles. We note that the doubly occupied nonbonding orbital of the lower $^1B_1$ state is localized on the nitrogen with the smaller CNC angle (Figure 4).

Potential energy curves based upon the HF energies of Table II for the b_{1u} mode of distortion are dipicted in Figure 5. Note that from an energetic point of view the loss of orbital symmetry is accompanied by a significant improvement in the single configuration description of the lowest $^1n\pi^*$ states. For the $^1B_{3u}$ state of D_{2h} pyrazine this improvement amounts to about 2 eV depending on geometry and basis set. The suggestion that the broken orbital symmetry presages a loss in the symmetry of the nuclear

(24) A. T. Amos and G. G. Hall, *Proc. R. Soc. London, Ser. A*, **263**, 483 (1961).
(25) K. K. Innes, J. P. Byrne, and I. G. Ross, *J. Mol. Spectrosc.*, **22**, 125 (1967).
(26) S. N. Thakur, and K. K. Innes, *J. Mol. Spectrosc.*, **52**, 130 (1974).

Table I. Coordinates[a] for Reference Geometries of Pyrazine

geometry symbol	selected internal coordinates	atom[b]	Y	Z
Opt ^1A_g	∠CNC = 112.4°	N_l, N_r	0.0	±2.7502
	CN = 1.379 Å	C_l, C_r	±2.1651	±1.3015
	CC = 1.377 Å	H_l, H_r	±3.9548	±2.3211
Opt $^1B_{3u}$	∠CNC = 116.4°	N_l, N_r	0.0	±2.7242
	CN = 1.389 Å	C_l, C_r	±2.2312	±1.3400
	CC = 1.418 Å	H_l, H_r	±4.0209	±2.3596
Opt $^1B_1$*	∠CNC = 115.9°	N_l, N_r	0.0	±2.7462
	CN = 1.447 Å	C_l, C_r	±2.3169	±1.2954
	CC = 1.371 Å	H_l, H_r	±4.1064	±2.3154
Opt $^1B_1$	$\angle C_lN_lC_l$ = 121.9°	N_l	0.0	2.5942
	$\angle C_rN_rC_r$ = 109.0°	N_r	0.0	−2.9312
	C_lN_l = 1.416 Å	C_l	±2.3399	1.2954
	C_rN_r = 1.491 Å	C_r	±2.2939	−1.2954
	CC = 1.371 Å	H_l	±4.1294	2.3154
		H_r	±4.0834	−2.3154
Exp	∠CNC = 115.1°	N_l, N_r	0.0	±2.6546
	CN = 1.334 Å	C_l, C_r	±2.1272	±1.3020
	CC = 1.378 Å	H_l, H_r	±3.9057	±2.3412

[a] All coordinates are in au (1 au = 0.5292 × 10^{-8} cm). The molecule is assumed to lie in the *yz* plane so that all *x* coordinates are 0.0 au. [b] The subscripts l and r refer to the left- and right-hand sides of the molecule (see Figure 1).

Table II. Hartree–Fock Excitation Energies[a,d] (eV) for $n\pi^*$ States of Pyrazine

geometry[b]	$^1B_{3u}$	1^1B_1	2^1B_1
Exp		4.04	4.04
Opt $^1B_{3u}$		3.84	3.84
Opt $^1B_1$*	5.77	3.85	3.85
[Opt $^1B_1$* + 1/2][c]		3.72	4.18
Opt $^1B_1$		3.72	4.64

[a] All energies are relative to the ^1A_g ground state in the Opt ^1A_g geometry. Using the unscaled exponents for hydrogen this energy is −262.56617 au (1 au = 27.2116 eV). [b] See Table I. [c] [Opt $^1B_1$* + 1/2] is the geometry at the half-way point along the Opt $^1B_1$* → Opt $^1B_1$ least motion pathway.[17] [d] See footnote 27 for a comparison of total energies calculated at various levels of sophistication.

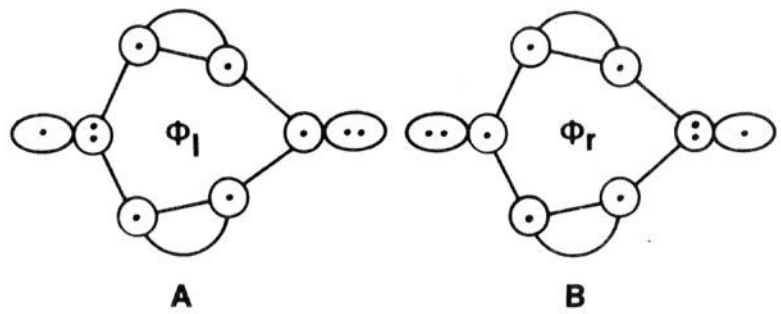

Figure 4. Leading resonance structures in the localized HF wave functions Φ_l and Φ_r, for the $n\pi^*$ states of C_{2v} pyrazine. Φ_l is the more stable of these two structures. In the valence-bond wave function Φ_l and Φ_r are allowed to combine. Φ_l is the leading contributor to the more stable of the pair of VB wave functions for the sense of distortion indicated in the figure.

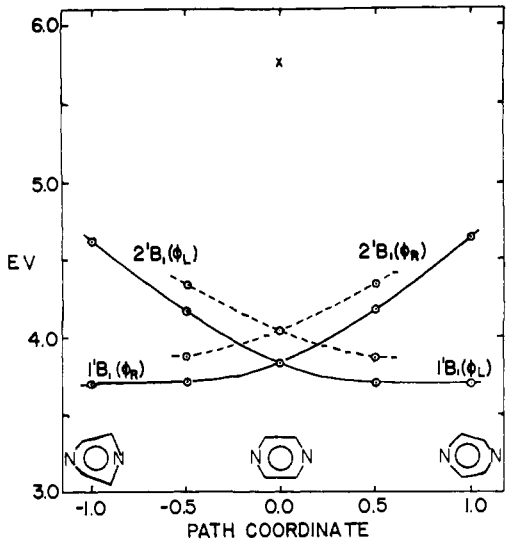

Figure 5. HF potential energy curves for b_{1u} distortions of pyrazine in the $^1B_1$ ($n\pi^*$) excited states. The energy is plotted relative to the energy of the ^1A_g ground state in the Opt ^1A_g geometry. Φ_r and Φ_l designate $^1B_1$ wave functions which are localized on the right- and left-hand nitrogens, respectively (see Figure1). The solid lines represent distortions along a "synchronous transit" path[17] between the Opt $^1B_1$* and $^1B_1$ geometries. From Table I, it can be seen that a path coordinate of 1 corresponds to $\Delta C_lN_lC_l \approx -\Delta C_rN_rC_r \approx 6.5°$. × represents the SRHF energy of the Opt $^1B_1$* geometry.

Table III. PSUHF (VB) Results for $n\pi^*$ States of Pyrazine[g]

		state					
		$^1B_{3u}$ (1^1B_1)[d]			$^1B_{2g}$ (2^1B_1)[d]		
geometry[a]	S_{12}[f]	E (eV)[b]	C_1[e]	C_2[e]	E (eV)[b]	C_1[e]	C_2[e]
Exp	−0.17	3.59	0.66	−0.66	4.67	0.77	0.77
Opt $^1B_{3u}$	−0.12	3.47	0.67	−0.67	4.33	0.75	0.75
Opt $^1B_1$*	−0.05	3.65	0.69	−0.69	4.07	0.73	0.73
[Opt $^1B_1$* + ½][c]	−0.05	3.59	0.91	−0.41	4.33	0.45	0.90
Opt $^1B_1$	−0.05	3.68	0.98	−0.19	4.70	0.23	0.97

[a] See Table I. [b] Energies relative to the HF energy of the ^1A_g state in its optimal geometry. Using unscaled exponents for hydrogen this energy is −262.56617 au. [c] See footnote *c*, Table II. [d] The $^1B_{3u}$ state correlates with 1^1B_1 and the $^1B_{2g}$ state with 2^1B_1 when the geometry is distorted from D_{2h} to C_{2v}. [e] C_1 is the coefficient of the structure with the excitation localized on the nitrogen with the larger CNC angle (Figure 1) while C_2 is the coefficient of the structure with the excitation localized on the nitrogen with the smaller CNC angle. [f] Overlap between localized solutions. [g] See footnote 27 for a comparison of total energies calculated at various levels of sophistication.

geometry is consistent with the C_{2v} minima in the SUHF potential curves (Figure 5). However, the SUHF solution suffers because, even though it is variationally better than the SRHF solution, it has lost the symmetry required of the exact wave function.

A more accurate description which recovers the lost symmetry at the D_{2h} geometry is obtained if the SUHF solutions are combined in a 2 × 2 valence bond calculation. Thus, a VB calculation at the D_{2h} geometry projects functions of appropriate B_{3u} and B_{2g} species from the pair of degenerate localized solutions.

The results of the PSUHF (or VB) calculations are presented in Table III and the corresponding potential energy curves are depicted in Figure 6. The $^1B_1$ curves from the PSUHF calculations no longer cross at the D_{2h} geometry as do their asymmetric counterparts from the SUHF calculations. Depending upon the D_{2h} geometry chosen, the splitting varies between 0.42 and 1.07 eV and the shape of the lower $^1B_1$ curve varies from a flat potential with a small barrier (~480 cm^{-1}) at the D_{2h} geometry to a flat potential with a minimum at the D_{2h} geometry. The relative position of the potential energy curve for the second $^1B_1$ state seems quite sensitive to the geometry chosen, but all curves are unambiguously single wells with minima at the D_{2h} geometries.

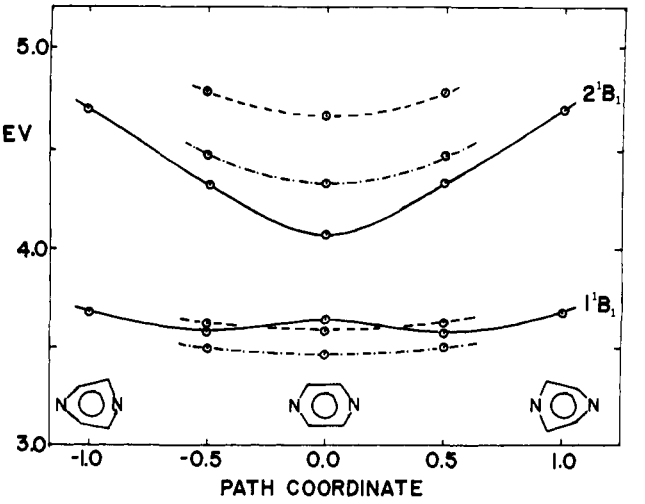

Figure 6. VB potential energy curves for $^1B_1$ states of pyrazine. The solid line is described in the caption to Figure 5. The dashed and dashed-dotted lines represent paths originating at the Exp and Opt $^1B_{3u}$ geometries, respectively. For each path coordinate along these latter paths the Cartesian coordinate changes are identical with those along the Opt $^1B_1$* → $^1B_1$ path.

Table IV. Configuration Interaction Energies[a,d] (eV) for $n\pi^*$ States of Pyrazine

	no. of ref	state	
geometry	configs	$^1B_{3u}$	1^1B_1
	A. MBS Results ((1+2) CI)		
Opt $^1B_1$*	1	0.90 (6100)[b]	0.33 (12 156)[c]
Opt $^1B_1$*	2	0.09 (12 042)[c]	
Opt $^1B_1$	1		0.00 (12 156)[c]
	B. DZ Results (Pol(1) CI)		
Opt $^1B_1$*	1	0.69 (6240)	0.16 (12 436)[c]
Opt $^1B_1$*	2	0.00 (12 322)[c]	
Opt $^1B_1$	1		0.00 (12 436)[c]

[a] Energies relative to energy of 1^1B_1 state in the Opt $^1B_1$ geometry. For the MBS (1+2) CI this energy is −259.5133 au. For the DZ-POL(1) CI this energy is −262.7461 au (1 au = 27.2116 eV). [b] Values in parentheses are the number of spin eigenfunctions generated for the state at the indicated level of CI. [c] A short linear extrapolation of less than 0.03 eV over a range of less than 1000 spin eigenfunctions was used to obtain this result. [d] See footnote 27 for a comparison of total energies calculated at various levels of sophistication.

Using the PSUHF results from the experimental geometry, the vertical excitation energies for the $^1B_{3u}$ and $^1B_{2g}$ states are now calculated to be 3.59 eV and 4.67 eV, respectively. The former figure is now slightly lower than the experimental vertical excitation energy (3.8–3.9 eV) which may be in part an artifact of recovering more correlation energy for the excited states than for the ground state.

The behavior of the VB wave function as a function of the distortion parameter is tabulated in Table III. At the D_{2h} geometry the $^1B_{3u}$ state has equal contributions from both of the resonance structures, Φ_l and Φ_r (Figure 1). However, as distortion proceeds along the b_{1u} mode, the resonance structure with the excitation localized on the nitrogen with the smaller CNC angle receives increasingly greater weight in the 2^1B_1 state.

The results of the CI calculations are presented in Table IV.[27] In principle, a fully correlated wave function within the confines of the designated orbital space should give the same energy ir-

(27) To illustrate the improvement in total energy with increasing sophistication of the approximate wave function, we note the following energies for the first $^1B_1$ state in the Opt $^1B_1$* geometry: −250.1920 au (SUHF–MBS), −259.5010 au (SUHF–MBS + (1+2)CI), −262.4247 au (SUHF–DZ), −262.4319 au (PSUHF–DZ), −262.7399 au (SUHF–DZ + POL(1) CI).

respective of whether a localized or full symmetry basis is used in the calculation. Since CI calculations (using a single reference configuration) at the various D_{2h} geometries continue to place the 1^1B_1 state below the $^1B_{3u}$ state, the superiority of the broken symmetry solutions continues to be affirmed even at this modest level of CI. Table IV shows that for the first $n\pi^*$ state the relative stability of the D_{2h} and C_{2v} geometries is problematical. For the MBS (1+2) CI the C_{2v} structure (1^1B_1 state, Opt $^1B_1$ geometry) is preferred by 0.09 eV (720 cm^{-1}) even when an extra "localizing" configuration (see Discussion) is included as a *second* reference in the CI calculation for the D_{2h} geometry ($^1B_{3u}$ state, Opt $^1B_1$* geometry). Similar conclusions follow from an analysis of the DZ-POL(1) results. Here the two-reference calculation for the D_{2h} geometry gives the same energy to within a hundredth of an eV as the single reference CI calculation for the C_{2v} geometry.

In summary, the PSUHF (VB) and CI results lead to the conclusion that, for the $^1B_{3u}$ state, the potential energy curve for the b_{1u} mode is either extremely flat or possesses a small barrier. In spite of their sophistication, the calculations do not allow an unambiguous answer to the question of whether the curve is a shallow single or shallow double well. It is clear that the potential energy curve for the second $n\pi^*$ state ($^1B_{2g}$) is characterized by a single minimum at the D_{2h} geometry as expected.

IV. Discussion

A. Localized Structures. As noted in the Results section, the lowest $n\pi^*$ excitation in C_{2v} pyrazine prefers the nitrogen with the larger CNC angle (see Figure 4). The nonbonding orbital localized on the nitrogen with the smaller CNC angle has more s character than the nonbonding orbital localized on the nitrogen with the larger CNC angle. Thus, when confronted with two options for placing three electrons into the two nonbonding orbitals, it is found that placing two in the orbital with high s character and one in the orbital with low s character is energetically more favorable; i.e., Φ_l of Figure 4 is more stable than Φ_r.

An analysis of the localized HF solutions for the D_{2h} geometry reveals that each such solution can be decomposed into a linear combination of two functions, one transforming according to the B_{3u} representation of the D_{2h} point group and the other according to B_{2g}. To a first approximation the localized nonbonding orbitals and localized π orbital can be represented in terms of the symmetry orbitals $n_+(a_g)$, $n_-(b_{1u})$, $\pi^*(b_{3u})$ and $\pi(b_{2g})$:

$$n_l = n_+(a_g) + n_-(b_{1u}) \qquad n_r = n_+(a_g) - n_-(b_{1u})$$

$$\pi_l = \pi^*(b_{3u}) + \pi(b_{2g}) \qquad \pi_r = \pi^*(b_{3u}) - \pi(b_{2g})$$

Expansion of the idealized configuration for the localized excitation on the left nitrogen then yields Thus, the localized HF solution

$$\begin{aligned}\Phi_l = \ldots n_r^2\pi_l^2 n_l\pi_r = \ldots &n_-(b_{1u})^2\pi(b_{2g})^2 n_+(a_g)\pi^*(b_{3u}) \\ &+ \ldots n_+(a_g)^2\pi^*(b_{3u})^2 n_-(b_{1u})\pi(b_{2g}) \quad B_{3u} \\ &+ \ldots n_+(a_g)^2\pi(b_{2g})^2 n_-(b_{1u})\pi^*(b_{3u}) \\ &+ \ldots n_-(b_{1u})^2\pi^*(b_{3u})^2 n_+(a_g)\pi(b_{2g}) \quad B_{2g}\end{aligned} \tag{1}$$

for the lowest $n\pi^*$ state of the D_{2h} geometry has effectively built in some correlation[28] by inclusion of the second configuration (the "localizing" configuration[29]), but at the expense of losing symmetry by inclusion of the third and fourth configurations ("symmetry-breaking" configurations[29]).

B. Second-Order Jahn–Teller (SOJT) Effect. A soft bending mode for pyrazine in its first $n\pi^*$ excited state can be viewed as the result of an SOJT effect.[11] Although our results are based upon variational calculations, they are consistent with arguments based upon second-order perturbation theory for either nondegenerate[11] or nearly degenerate[30] zeroth order states. Using a perturbation expansion in the vibration coordinate $Q(b_{1u})$ and ignoring all couplings except the one which is induced between the lowest B_{3u} and B_{2g} states, the quadratic force constant for the b_{1u} mode is approximated by

$$k = \langle\psi_{B_{3u}}|\partial^2 H/\partial^2 Q(b_{1u})|\psi_{B_{3u}}\rangle - \frac{2|\langle\psi_{B_{2g}}|\partial H/\partial Q(b_{1u})|\psi_{B_{3u}}\rangle|^2}{(E_{B_{2g}} - E_{B_{3u}})} \tag{2}$$

where $\psi_{B_{3u}}$ and $\psi_{B_{2g}}$ are exact electronic wave functions for the D_{2h} geometry. Since $\partial H/\partial Q(b_{1u})$ transforms like b_{1u}, the second integral does *not* vanish by symmetry and the possibility for a negative quadratic force constant and hence a double-well potential arises. Since bending force constants, even in the absence of SOJT coupling, are rather small (e.g., $\langle\psi_{B_{3u}}|\partial^2 H/\partial^2 Q(b_{1u})|\psi_{B_{3u}}\rangle$ is expected to be small), there is a strong possibility that they will become negative when the coupling is taken into account. By way of contrast, bond stretching force constants are usually rather large, and hence, SOJT effects are not as likely to result in negative force constants for stretching modes.[11b]

The strength of this SOJT coupling for the first $n\pi^*$ state was suggested by the symmetry breaking at the HF level. At the HF level the coupling between the B_{3u} and B_{2g} states is induced by correlation effects (see discussion of eq 1), while from the point of view of perturbation theory an analogous coupling is induced by a perturbation of the nuclear attraction term of the electronic Hamiltonian (see Eq 2). In both cases the strength of the coupling depends upon the proximity of the electronic states of different symmetry.

C. Correlation Effects. As noted above, localization at the HF level effectively correlates the $^1B_{3u}$ wave function at the expense of lost symmetry.[28] The configuration interaction calculations on the $^1B_{3u}$ state are consistent with the heavy weight given to the "Localizing" configuration in eq 1. Thus, when the two B_{3u} configurations of eq 1 were used as references in the POL-CI reported in Table IV, the coefficient of the leading configuration had a magnitude of 0.87 while the "localizing" configuration was weighted by a large coefficient of magnitude 0.30. No other coefficient had a magnitude larger than 0.10. This critical "localizing" configuration is related to the leading configuration by a double excitation of the form $n_- \rightarrow n_+$, $\pi \rightarrow \pi^*$.[4] Inclusion of the "localizing" configuration effectively cancels ionic resonance structures of the form

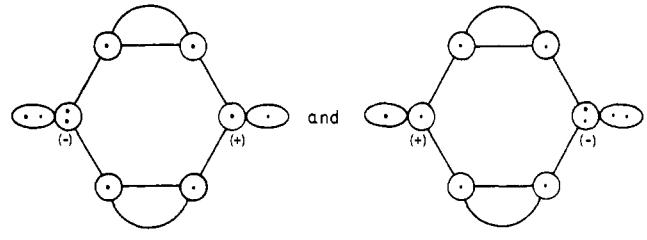

and hence provides for a kind of longitudinal correlation.

D. Comparison with Experiment. The predicted distortion of $n\pi^*$ excited-state potentials along b_{1u} vibrational modes of pyrazine should have noticeable and significant consequences for the spectroscopy and photochemistry of this molecule. There are, in fact, three pieces of empirical evidence that are consistent with the foregoing theoretical description of the excited state.

(1) In both the vapor[13] and the crystal[14] two-photon spectra, one of the strongest false origins is of b_{1u} symmetry and has a one- or two-member progression in the totally symmetric 6a mode built upon it.[31] The b_{1u} false origin is found to be 636 cm^{-1} above the single photon-allowed 0–0 band.[13,14] There are four vibrational modes of b_{1u} symmetry. These have ground-state frequencies of 1021, 1135, 1484, and 3066 cm^{-1}.[25] This means that there has

(28) We are somewhat arbitrarily defining correlation energy as the difference between the best SRHF energy and the true energy. The best HF energy corresponds to a broken symmetry solution and the improvement over the SRHF result is thus attributed to correlation.

(29) It seems appropriate to label this second configuration as the "localizing" configuration in the sense that when this configuration is added to the leading configuration of B_{3u} symmetry, it cancels ionic resonance structures which delocalize the excitation (see text, section, IVC).

(30) R. M. Hochstrasser and C. A. Marzzacco, in "Molecular Luminescence", E. C. Lim, Ed., W. A. Benjamin, New York, 1969, p 631.

(31) These symmetry assignments are based upon two-photon polarization measurements and clearly reveal the B_{2g} ($B_{3u} \times b_{1u}$) vibronic symmetry. The fact that the totally symmetric 6a mode has the identical frequency as observed in the one-photon spectrum[14] rules out the possibility that this false origin is the true origin of a second transition to the $n\pi^*$ state of B_{2g}.

been a drop of at least 40% in the frequency of the spectroscopically active b_{1u} mode in the B_{3u} excited state. This decrease in frequency requires an excited-state potential surface that is much flatter and more distorted along a b_{1u} mode than is the case for the ground state. The failure to see any vibronic band of reasonable intensity at 2×636 cm^{-1} [15] in the one-photon spectrum or at 3×636 cm^{-1} [14] in the two-photon spectrum also supports the existence of a strongly anharmonic excited-state potential. These spectroscopic data are consistent with a flat, or shallow, double-well potential along a b_{1u} normal coordinate.

(2) In D_{2h} geometry, the molecule retains a center of symmetry which would be lost if the molecule suffered a permanent distortion to C_{2v}. Also lost in this distortion are the mutually exclusive one- and two-photon selection rules for transitions from the ground, $^1A_{1g}$, state to the lowest $n\pi^*$, $^1B_{3u}$, state. (In C_{2v} geometry these become $^1A_1$ and $^1B_1$, respectively.) In fact, the strongly allowed 0–0 transition in the one-photon spectrum is not observed in the two-photon spectrum of either the vapor[13] or the neat crystal.[14] This is strong evidence for D_{2h} geometry in the lowest $^1B_{3u}$ $n\pi^*$ state. At most an inversion barrier that is lower than the zero-point energy of the b_{1u} vibrational mode ($^1/_2 \times 636 \approx 300$ cm^{-1}, see part 1 above) is possible.

(3) Recent studies by one of us[15] on the hydrogen-bonding properties of the excited $n\pi^*$ states of the azines provide an additional insight into the nature of those states. Pyrazine in the ground state is able to form either a singly hydrogen-bonded complex or a doubly hydrogen-bonded complex with fluorinated alcohols. At low alcohol concentrations, a new, vibronically structured $n\pi^*$ absorption spectrum appears which is assigned to singly hydrogen-bonded pyrazine. The 0,0 band is shifted only 350 cm^{-1} to higher energy from its position in free pyrazine, so that the hydrogen bond is only destabilized by this amount in the excited $n\pi^*$ state relative to the ground state. The existence of vibronic structure in the $n\pi^*$ absorption spectrum of the complexed pyrazine and the appearance of a new corresponding fluorescence imply that the singly hydrogen-bonded species is stable in the lowest $^1n\pi^*$ state.

These data are consistent with a description of the lowest $n\pi^*$ excited state which has the excitation localized at the end of the molecule that is not hydrogen bonded. One would expect a much greater weakening of the excited-state hydrogen bond (and a larger shift in the $n\pi^*$ absorption spectrum) if the excitation were more delocalized. Preliminary calculations suggest that the presence of a hydrogen bond at the left end of the molecule will indeed lead to differential stabilization of the resonance structure in which two nonbonding electrons remain on the left while the excitation is localized on the right.

At higher alcohol concentration, the $n\pi^*$ absorption spectrum becomes structureless and shifts by at least 2000 cm^{-1} to higher energy. This spectrum is assigned to doubly hydrogen-bonded pyrazine. The fluorescence, however, remains essentially the same as that which was assigned to the singly hydrogen-bonded species. These data suggest that although ground-state pyrazine can form a doubly hydrogen-bonded complex, only the singly bonded species is stable in the lowest $n\pi^*$ singlet excited state (at least during its lifetime).

The apparent instability of the doubly hydrogen-bonded $n\pi^*$ state is consistent with the ready compliance of the lowest $n\pi^*$ state to any perturbation which will reduce the nuclear geometry from D_{2h} to C_{2v}. In this instance the reduction is accomplished by breaking one of the hydrogen bonds in the symmetrically hydrogen-bonded species, thereby localizing the excitation at the same end as the departed proton donor.

The PSUHF calculations predict that the second $n\pi^*$ electronic state (i.e., the $^1B_{2g}$ state) in pyrazine should lie 1.1 eV (8900 cm^{-1}) above the lowest $^1B_{3u}$ state (see Exp geometry in Table III). This splitting is quite similar to the vertical excitation energies reported by Wadt and Goddard[4b] for their CI calculation (1.30 eV). Single configuration SRHF calculations generally predict a splitting of about 2.3 eV, but the introduction of configuration interaction reduces it to 1.4 eV.[10]

Very little empirical evidence is available for the existence or location of a state of $^1B_{2g}$ symmetry in pyrazine. Esherick, Zinsli, and El-Sayed published[14] their two-photon spectrum of pyrazine covering a spectral range 3600 cm^{-1} above the origin and found no evidence for a state of B_{2g} symmetry in that range. Using triplet–triplet absorption Inoue, Webster, and Lim[32] have measured the splitting of the $^3B_{3u}$ and $^3B_{2g}$ in pyrazine to be $\sim$1.5 eV. Our theoretical calculations[4] indicate that the splitting of the triplet and singlet $n\pi^*$ states should be comparable.

Studies of hydrogen-bonded pyrazine[15] have revealed the presence of an electronic transition which may be the $^1B_{2g}$ state. This band appears as a broad, weak feature, which increases in intensity with increasing alcohol concentration. The position also shifts gradually to higher energy, as an $n\pi^*$ transition should, from under the high-energy side of the $^1B_{2u}$ $\pi\pi^*$ transition as alcohol is added. Since this transition is observed only when pyrazine is hydrogen-bonded, determining its position in pyrazine itself is difficult. By making various assumptions concerning the solvent shift of this transition, we can set limits on the energy of the vertical excitation of between 5.3 and 5.5 eV above the ground state. This leads to a vertical splitting between this state and the $^1B_{3u}$ state of 1.3–1.5 eV. The splitting of the adiabatic energies will, of course, be smaller than this by an unknown amount. These figures are in reasonable agreement with the calculated splitting of 1.1 eV, and support the notion that the splitting of the two $n\pi^*$ states is large ($\sim$1 eV) rather than small ($\sim$0.1 eV) as previously thought.[33]

V. Conclusions

The experimental evidence is consistent with our proposed theoretical description. The lowest $^1B_{3u}$ $n\pi^*$ state of pyrazine is best represented by the in-phase combination of two strongly localized valence-bond structures. The potential curve for this excited state is strongly anharmonic along at least one b_{1u} normal mode. The spectroscopic evidence does not support a model in which there is a barrier greater than the zero-point energy of the b_{1u} mode ($\sim$300 cm^{-1}), but it does not rule out the presence of a low barrier. The finding that symmetry breaking in single-configuration SCF states may imply anharmonic distortions of the potential surface provides new insights into what is generally referred to as vibronic coupling between electronic states. The extent to which these ideas are generalizable in medium-sized polyatomic molecules awaits further calculations which are now in progress.

Acknowledgment. D.A.K. acknowledges the helpful advice and computational assistance provided by Professor Thomas A. Halgren. This work was performed under the auspices of the Department of Energy.

Registry No. Pyrazine, 290-37-9.

(32) A. Inoue, D. Webster, and E. C. Lim, *J. Chem. Phys.*, **72**, 1419 (1980).
(33) D. K. Kearns and M. A. El-Bayoumi, *J. Chem. Phys.*, **38**, 1508 (1963).